Resonance Raman Spectroscopic Study of Alumina-Supported Vanadium Oxide Catalysts with 220 and 287 nm Excitation†

Hack-Sung Kim and Peter C. Stair*

Department of Chemistry, Center for Catalysis and Surface Science and Institute for Catalysis and Energy Processes, Northwestern University, Evanston, Illinois 60208, and Chemical Sciences and Engineering Division, Argonne National Laboratory, Argonne, Illinois 60439

Received: December 14, 2008

We present detailed resonance Raman spectroscopic results excited at 220 and 287 nm for alumina-supported VO_x catalysts. The anharmonic constant, harmonic wavenumber, anharmonic force constant, bond dissociation energy, and bond length change in the excited state for double bonded V═O and single bonded V−O were obtained from fundamental and overtone frequencies. Totally symmetric and nontotally symmetric modes could be discerned and assigned on the basis of the overtone and combination progressions found in the resonance Raman spectra. Selective resonance enhancement of two different vibrational modes with two different excitation wavelengths was observed. This allowed us to establish a linear relationship between charge transfer energy and VO bond length and, consequently, to assign the higher-energy charge transfer band centered around 210−250 nm in the UV−vis spectra to the V═O transition.

Introduction

Whereas significant progress has been made in understanding supported metal oxide catalysts and catalysis, the detailed knowledge and understanding of surface molecular structures, structure−reactivity relationships, and support effects,[1,2] have remained unresolved. This is due in part to the intrinsic difficulties associated with (1) the poorly defined structures of support oxides and metal oxides dispersed on the surface where the complicated gas/solid catalytic reactions occur, (2) the requirement of highly sensitive experimental techniques for probing metal oxides with low surface density (e.g., less than monolayer coverage), and (3) the dependence of reactivity on the conditions of temperature, gas pressure and velocity, gas and solid concentrations, and so on. The role of vibrational spectroscopy in this regard is to provide molecular-level information on the nature of the bonding in these species.

The core bonds in supported transition-metal (M) oxide catalysts that affect the heterogeneous catalytic reactions are the M═O and M−O−X (X = M, Al, etc.) bonds.[3−5] Supported vanadium oxide is the most extensively studied catalyst among supported metal oxide catalysts.[6] The V═O and V−O vibrations are frequently difficult to observe by IR spectroscopy because metal oxide supports strongly absorb at energies below ∼1100 cm^{-1}, where the core vibrational bands appear.[3,7] In Raman spectra excited at visible wavelengths, the V═O stretch centered at ∼990−1030 cm^{-1} (including V_2O_5 at 995 cm^{-1}) is quite intense, but the V−O stretch at ∼850−960 cm^{-1} is typically weak and even undetectable at low V surface density.[8−11] Therefore, whereas V═O bands can be easily observed with either visible or UV excitation, V−O bands require the enhancement of resonance Raman to be observed at low V surface density. With resonance enhancement, the detection sensitivity of Raman spectroscopy enormously increases. For example, intense V−O stretching vibrations have been observed[10] using deep UV excitation of the catalysts with extremely low V concentrations, where only isolated, monomeric species exist.

Overtone and combination bands provide additional information about molecular properties. They are generally intense in infrared spectra but very weak in Raman spectra.[12] The overtone and combination bands of V−O and V═O vibrations have been reported in IR spectroscopy,[13−18] but have never, to our knowledge, been reported using normal ("off-resonance" or "nonresonance") Raman spectroscopy. In normal Raman scattering, the intensities of overtones or combinations are determined by the second derivatives of the polarizability components with respect to the equilibrium normal coordinate, Q_k, such as $(\partial^2\alpha_{xy}/\partial Q^2_k)_0$, which are usually very small relative to the corresponding first derivatives, $(\partial\alpha_{xy}/\partial Q_k)_0$.[19] However, under the proper conditions, overtone and combination bands can be observed using resonance Raman spectroscopy. Extensive studies have been made of overtones and combinations in small molecules or ions[20,21] and biomolecules[22,23] by resonance Raman spectroscopy. UV Raman or resonance Raman spectroscopic techniques have been applied to study heterogeneous catalysts only relatively recently.[24,25] The group of Can Li at the Dalian Institute of Chemical Physics has observed overtones of Mo═O and Mo−O in MoO_x catalysts by resonance Raman spectroscopy excited at 244 and 325 nm,[26,27] but the discussion is far from detailed. Here we present the first extensive analysis of resonance Raman spectra excited at 220 and 287 nm for alumina-supported vanadium oxide catalyst materials. As we shall see in the present article, the observation of overtone and combination bands by resonance Raman spectroscopy can be a powerful tool for assigning the electronic transitions observed in UV−vis absorption spectra because of the direct link to the VO stretching vibrations that are enhanced.[28,29]

Experimental Section

Sample Preparation. The preparation method is described in detail elsewhere.[10] Briefly, VO_x supported on θ-Al_2O_3 (Johnson Matthey, UK, BET Surface area = 101 m^2/g) has been

† Part of the "George C. Schatz Festschrift".

* Corresponding author. E-mail: pstair@northwestern.edu. Fax: 847-467-1018.

10.1021/jp811019c CCC: $40.75
Published on Web 03/03/2009

TABLE 1: VO_4-Associated Fundamentals in O=V(OH)$_x$(OAl)$_y$ ($x = 0$ and 1, $y = 3 - x$) Structures Belonging to the Point Groups of C_{3v} or C_s and the Correlation[a]

C_{3v} point group		C_s point group	
Symmetry	Vibrational mode	Vibrational mode	Symmetry
A_1, symmetric	ν_1, V=O stretching	ν_1, V=O stretching	A′, symmetric
	ν_2, V-O stretching in VO_3	ν_2, V-O stretching in VO_2	
		ν_3, V-O stretching in VOH	
	ν_3, VO_3 deformation	ν_4, VO_2 deformation	
		ν_5, O=V-O_2 deformation	
		ν_6, HO-V-O_2 deformation	
E, non-symmetric	ν_4, V-O stretching	ν_7, V-O stretching in VO_2	A″, asymmetric
	ν_5, VO_3 deformation	ν_8, OH-V=O deformation	
	ν_6, O=VO_3 rocking	ν_9, OH-V-O_2 deformation	

[a] The Al-associated vibrations of Al−O stretching and Al−O−V deformation are not included. The degenerate E mode of C_{3v} splits into one symmetric (A') and one asymmetric (A'') mode of C_s. All fundamentals in C_{3v} and C_s are active in both the IR and Raman. Some of approximate V−O stretching normal modes in C_{3v} structure are shown Figure 5.

prepared by incipient wetness impregnation using ammonium metavanadate. The VO_x/θ-Al_2O_3 samples with surface VO_x densities of 0.16 V/nm^2, 1.2 V/nm^2, and 4.4 V/nm^2 (hereafter referred to as 0.16V, 1.2V, and 4.4V, respectively) were chosen for this study. The 0.16V corresponds to about 2% of a monolayer and possesses predominantly isolated VO_x in tetrahedral coordination.[10] Similarly, 1.2V and 4.4V correspond to 15% and 55% monolayer coverage, respectively, and possess a mixture of monomeric and polymeric VO_x. After impregnation, the samples were dried and calcined at 823 K. 0.16V is the most uniform sample, as evidenced by the narrowest Raman band and the absence of bulk V_2O_5, as shown later.

Raman Spectroscopy. Raman spectra were recorded with a triple spectrometer (Princeton Instruments Acton, Trivista 555) equipped with a liquid-nitrogen-cooled CCD detector using 220 and 287 nm laser excitation from a broadly tunable laser (Coherent Indigo-S). The laser power delivered to the sample was 1 mW at 220 nm excitation and 5 mW at 287 nm excitation. The Raman shift was calibrated with a Hg lamp and several frequency standards such as cyclohexane and chloroform. The accuracy of absolute Raman shifts is approximately $\pm$ 1 cm^{-1}.

All Raman spectra were obtained at room temperature under dehydrated or hydrated conditions. The sample was dehydrated in a fluidized bed reactor[30] in flowing 5% O_2/N_2 (60 mL/min) at 823 K for 2 h and then cooled to room temperature in flowing 5% O_2/N_2. Raman spectra were then recorded at room temperature in flowing He ($\sim$100 mL/min). Hydrated samples were obtained by exposing the dehydrated sample to room-temperature air environment. Raman spectra were then recorded at room temperature in air.

Results and Discussion

A primary purpose of this research is to better understand the relationship between the molecular structures of vanadium oxides supported on alumina and their vibrational and electronic properties. To facilitate the presentation and discussion of the Raman spectroscopy results, we begin with a brief review of the monomeric structures of surface vanadium oxides.

Monomeric Structures of Vanadium Oxide on Alumina Surface. ***Previous Studies on the Structures.*** EXAFS and ^{51}V NMR spectra[31−36] showed that the molecular structure (both hydrated and dehydrated) of VO_x on alumina at low V surface coverage has distorted-tetrahedral symmetry with one short V=O bond and three long V−O bonds, presumably[31] the three V−O−Al bonds. UV−vis spectra also show evidence of tetrahedral symmetry for both hydrated and dehydrated VO_x on alumina.[10]

Although VO_4 with three V−O−S (S=Al, Si, etc.) bonds (i.e., three basal, bridging oxygen atoms coordinated to the support with ca. C_{3v} symmetry) is believed to be the most likely structure, especially under dehydrated conditions,[5,6,31] the EXAFS and ^{51}V NMR results also suggest a partial contribution from VO_4 with only one or two V−O−S bonds. For example, a broad NMR band due to four-fold VO_x is consistent with an inhomogeneous environment that possibly includes differing numbers of nonbridging oxygen atoms.[34] A VO_4 structure with a single V−O−S has been assumed in earlier theoretical calculations,[37] and a recent EXAFS study concluded that it can be formed under dehydrated conditions.[35] A hydrated tetrahedral structure with two V−O−Al bonds, $(Al-O)_2V=O(OH)$, (C_s symmetry) where OH is directly coordinated to the V atom, has also been identified by EXAFS for VO_x on alumina.[38] The formation of two V−O−Al bonds from three V−O−Al bonds due to hydration may be similar to models[39,40] suggested for Mo and W, where M−OH and Al−OH are formed from M−O−Al and H_2O.

Structures and Existing Band Assignments. DFT calculations[41] show that for dehydrated monomeric VO_x on θ-alumina, the conventional tridentate structure with three V−O−Al bonds is the most stable in the sequence, tridentate (three V−O−Al bonds, C_s symmetry, not C_{3v}) > bidentate (two V−O−Al bonds, pseudo C_{3v} symmetry) > molecular (two V−O−Al bonds, C_s symmetry). All three structures are similar to previously proposed structures[5,6,31] but differ somewhat in the details.

In this work, we focus on the analysis of the higher frequency vibrations, >850 cm^{-1}. For C_{3v} and C_s structures, where the basal oxygen atoms are coordinated to Al atoms and neglecting the low frequency Al-associated Al−O stretching and Al−O−V deformation modes, the VO_4 units have six and nine fundamental vibrations, respectively. The symmetry species,[42,43] Γ (C_{3v}) = $3A_1 + 3E$ and Γ (C_s) = $6A' + 3A''$, fundamental vibrations, and the correlation between C_{3v} and C_s point groups are included in Table 1.

The preresonance Raman spectra for dehydrated monomeric 0.16V VO_x on θ-alumina excited at three different visible wavelengths showed three distinct V=O Raman bands that match well the positions of the three V=O bands obtained by DFT calculations[41] for the three structures. Therefore, three monomeric structures appear to be present on the surface of dehydrated VO_x on θ-alumina. The two lower-frequency V=O Raman bands of the three were detected by 220 and 287 nm excitation on 0.16V (Figures 1 and 2).[44] Consequently, the composite band observed for 0.16V was fitted by two Lorentzian peaks. The width of the observed V=O band for 0.16V is the

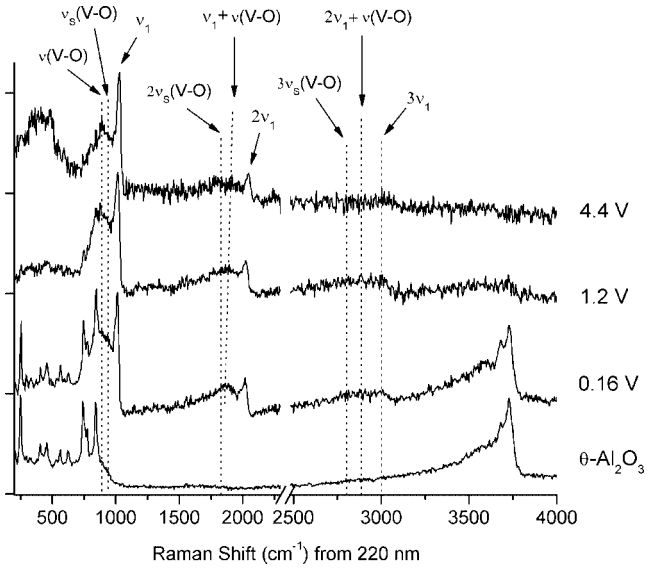

Figure 1. Resonance Raman spectra excited at 220 nm recorded under the dehydrated conditions for θ-Al_2O_3 and X (V/nm^2) on θ-Al_2O_3 (X = 0.16, 1.2, and 4.4). Spectra were obtained at room temperature under He flow. ν_1 denotes the symmetric V=O stretching mode, ν_S(V=O).

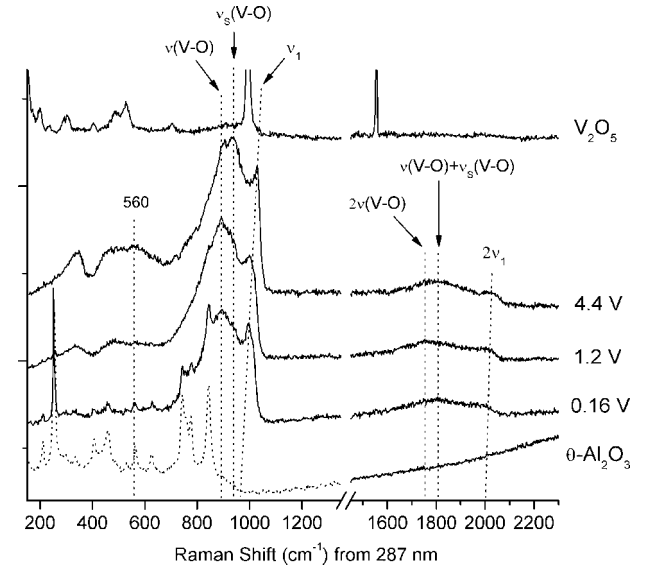

Figure 2. Resonance Raman spectra excited at 287 nm recorded under the dehydrated conditions for θ-Al_2O_3, 0.16V, 1.2V, and 4.4V. The V_2O_5 spectrum excited at 287 nm was obtained under room-temperature ambient air conditions. All other spectra were obtained at room temperature under He flow.

narrowest, which indicates that 0.16V is the most uniform sample, whereas 4.4V includes[10] a small amount of bulk V_2O_5. Assuming that the width of each component is independent of vanadium loading, the fitting of V=O bands for 1.2V and 4.4V resulted in three components. The fitted results are summarized in Table 2.

The observed V=O bands shift to higher wavenumber as vanadia surface density increases (i.e., 1014, 1017, and 1028 cm^{-1} for 0.1V, 1.2V, and 4.4V, respectively). The highest-frequency component V=O bands at 1021 and 1031 cm^{-1} for 1.2V and 4.4V, respectively, are assigned to V=O bonds associated with polymeric (five- or six-coordinate) VO_x species on θ-alumina on the basis of the presence of symmetric V−O−V stretching Raman bands centered at ∼560 cm^{-1} (Figure 2). The presence of polymeric species is also supported by the UV−vis absorption spectra for 1.2V and 4.4V, as

TABLE 2: Observed V=O Fundamental and Lorentzian Fitted Component Bands[a]

sample	observed, Raman	fitted positions and relative intensities of Lorentzian component bands	
0.16V	1014	997, 1015	1, 2.7
1.2V	1017	991, 1007, 1021	1, 1.6, 2.4
4.4V	1028	993, 1016, 1031	1, 2.9, 4.5

[a] Observed bands are taken from the Raman spectra excited at 220 nm shown in Fig 1. All positions are in cm^{-1}.

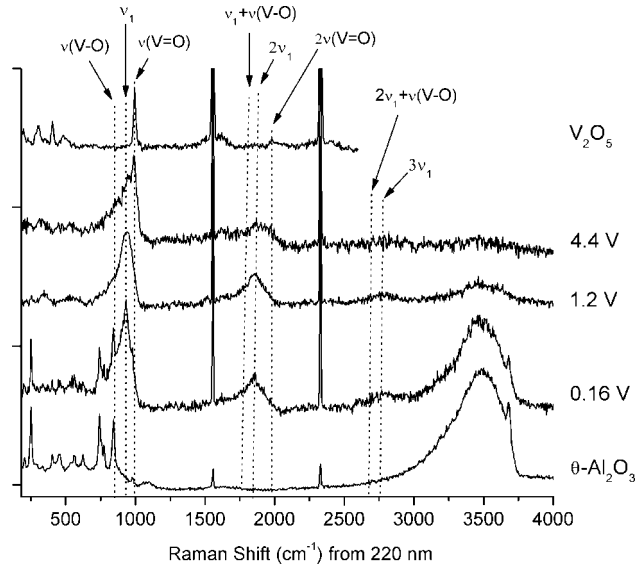

Figure 3. Resonance Raman spectra excited at 220 nm recorded under the hydrated conditions for θ-Al_2O_3, 0.16V, 1.2V, 4.4V, and V_2O_5. All spectra were obtained under room-temperature ambient air conditions. Here ν_1 denotes the symmetric V−O stretching mode, ν_S(V−O).

discussed later. With 514.5 nm excitation, two V=O Raman bands for dehydrated 4V on γ-alumina prepared by the impregnation method have been observed at 1009 and 1026 cm^{-1}.[45] These bands correspond to the two higher-frequency V=O components for 4.4V at 1016 and 1031 cm^{-1}, respectively, although our assignment (monomeric and polymeric, respectively) is the opposite of ref 45.

Resonance Raman Spectra in the 200−4000 cm^{-1} Region. The Raman spectra for θ-Al_2O_3 and vanadia supported on θ-Al_2O_3 (Figures 1−3) make possible the identification of VO_x-associated overtones and combinations as well as fundamentals. The resonance Raman spectra excited at 220 or 287 nm (Figures 1−3) are in general agreement with previously published spectra[10] excited at 244 and 488 nm, but the new spectra include additional features such as overtones, combinations, and OH stretching.

V=O Resonance Enhancement with 220 nm Excitation, Dehydrated. We define ν_1 as the highest-frequency VO stretching mode for both dehydrated and hydrated conditions. Therefore, ν_1 is ν_S(V=O) when V=O is present. (See Table 1 for assignments.) The Raman spectra from all of the vanadia samples are found to depend significantly on the excitation wavelength. With 220 nm excitation, adjacent to the electronic absorption band maximum at ∼210 nm, the Raman spectra shown in Figure 1 for dehydrated vanadia samples are characterized by a significant enhancement of the intensity for the symmetric V=O stretching mode, ν_S(V=O) or ν_1, and by the appearance of an overtone progression in ν_1 up to $3\nu_1$, a combination progression in $\nu_1 + \nu$(V−O), and an overtone progression in ν_S(V−O) up to $3\nu_S$(V−O).

TABLE 3: Observed Resonance Raman Data Excited at 220 nm and the Parameters for V=O and V−O Stretching Modes of VO_x on θ-Alumina under the Dehydrated and Hydrated Conditions and of Related Compounds[a]

sample	assignment	fundamental, width (W_F)	1st overtone, width (W_O)	$I_{2\nu 1}/I_{\nu 1}$[c]	W_O/W_F	2nd overtone	$\omega_e x_e$[d]	ω_e	D_0	f_e	f	VO distance (Å)[e]
0.16V, dehyd	ν_S(V=O): A_1, C_{3v} and A',	1014, 38	2019, 58	0.5	1.5	3003	6.5	1028	480	7.57	7.37	1.59
1.2V, dehyd	C_s: denoted as ν_1	1017, 47	2024, 72	0.4	1.5	3007	7.3	1032	430	7.64	7.42	1.59
4.4V, dehyd		1028, 38[b]	2045, 50[b]	0.3	1.3	3041	7.2	1043	450	7.80	7.58	1.58
0.16V, hyd	ν_S(V−O) in V=O···H and	933, 104	1858, 141	0.5	1.4	~2765	5.7	945	466	6.40	6.24	1.63
1.2V, hyd	V−O−Al, A', C_s: denoted as ν_1	938, 141	1861, 164	0.5	1.3	~2785	4.8	947	550	6.43	6.31	1.63
0.16V, 1.2V, 4.4V, hyd	ν(V−O): A'', C_s, asymmetric	~850										
V_2O_5	ν_S(V=O), A_g, D_{2h}	995	1980	0.1							7.10	1.60
$VOCl_3$/ $VOBr_3$[f]	ν_S(V=O), A_1, C_{3v}	1035/1025	2061								7.70/7.64	
VO[g]	ν_S(V=O), A_1, $C_{\infty v}$						4.9	1011	618			1.59
VO_4^{3-}[f]	ν_S(V−O), T_d	870									5.16	

[a] Band position, width (full width at half-maximum), harmonic frequency (ω_e), and anharmonic constant ($\omega_e x_e$ is equal to x_{11} for ν_1) are in cm^{-1}. Dissociation energy, D_0 estimated from the Raman data is in kJ/mol. Harmonic and anharmonic force constant (f and f_e, respectively) estimated from the Raman data are in mdyn/Å. [b] Widths are not less than those of 1.2V if the weak, lowest-frequency component band at ~993 cm^{-1} is included in width. The contribution from the component band is not included because its height is lower than half-maximum. [c] Intensity ratio. Intensities were obtained from products of the peak heights and widths. [d] Obtained from the plot of $\nu_1(n)/n$ versus n (Figure 6). [e] Estimated from the correlation described in ref 81 except for VO. [f] Taken from ref 72. [g] Taken from ref 89.

The intensity ratio of the V=O fundamental, ν_1 to the V−O fundamental, $I(\nu_1)/I(\nu_{V-O})$, obtained with 220 nm excitation is about two times higher than with 287 nm excitation (Figures 1 and 2) and much higher than with visible excitation.[41] The intensity of V−O stretching fundamentals is also enhanced with 220 nm excitation, but not as much as ν_1. This indicates that V=O is selectively enhanced by 220 nm excitation.

The assignment of overtones and combinations is quite straightforward on the basis of the examination of the spectral region where the bands are expected to occur. The intensity of the first overtone, $2\nu_1$, is weaker than the fundamental, ν_1, and the second overtone, $3\nu_1$, is weaker than the first overtone, $2\nu_1$. The overtone bands are also broader than the fundamentals. These observations are consistent with resonance-enhancement by the Albrecht A term,[46,47] where ν_1 is a totally symmetric mode with a large displacement of the V=O bond length in the excited state.[19,21,23,28] The calculation of the V=O bond length change will be described later.

Nontotally symmetric modes generally have no A-term contribution because there is no displacement of the potential curve in the excited state and do not show overtone progressions.[28] The absence of overtones in ν(V−O) combined with the appearance of an overtone progression in ν_S(V−O) up to $3\nu_S$(V−O) (Figure 1) suggests that ν(V−O) is most likely a nonsymmetric mode and ν_S(V−O) is a symmetric V−O stretching mode. In combination with DFT calculations,[41] we assign ν(V−O) centered at 892 cm^{-1} to ν_7, A'' (asymmetric) in the C_s, tridentate and ν_4, E (nonsymmetric) in the C_{3v}, bidentate structures. (See Table 1.)

A weaker combination progression of $\nu_1 + \nu$(V−O) induced by the progression-forming ν_1 mode is also evident in the resonance Raman spectra up to $2\nu_1 + \nu$(V−O) (Figure 1). When a strong overtone progression is observed, it is common to observe secondary (combination-band) progressions, which can be explained by the 2D Franck−Condon factors.[28] Similar progressions in combinations of totally symmetric and asymmetric stretching modes have been observed for MnO_4^-, CrO_4^{2-}, and $AuBr^-$.[20,48,49]

Although the presence of ν_S(V−O) centered at ~940 cm^{-1} is uncertain in the fundamental region because ν_S(V−O) and ν(V−O) are overlapping and broad (~200 cm^{-1}), it is quite clear in the overtone region where the difference in position of ν_S(V−O) and ν(V−O) increases by a factor of two and three (Figure 1). The presence of a symmetric V−O stretching mode, ν_S(V−O), at ~940 cm^{-1} is expected from group theory (Table 1) and consistent with theoretical calculations[2,50] and Raman band assignments.[31] Further evidence can be found in the resonance Raman spectra excited at 287 nm (Figure 2), where the V−O modes are selectively enhanced and thus the 940 cm^{-1} band is better resolved and a ν(V−O) + ν_S(V−O) combination band (892 + 940 cm^{-1}) centered at ~1805 cm^{-1} appears. For comparison, under hydrated conditions where V=O modes are absent, a fundamental and overtones of ν_S(V−O) centered at ~938 cm^{-1} strongly appear in the resonance Raman spectra excited at 220 nm (Figure 3).

In combination with DFT calculations[41] for the three dehydrated structures, we assign the 940 cm^{-1} band to the symmetric V−O stretching, ν_S(V−O), in VOH···$O_{surface}$ (ν_3, A' in C_s, molecular), where the V−O bond length is 1.63 Å, the shortest V−O distance among all V−O's in the three structures. It may also be assigned to ν_S(V−O) in $V(OAl)_2$ (ν_2, A' in C_s, tridentate), where the V−O bond length is 1.71 to 1.74 Å, that is, the second shortest V−O bond.

Tran et al.[51] assigned a Raman band at 977 cm^{-1} for vanadia in a silica xerogel to the basal plane V−O stretching in pseudotetrahedral O=V−(O−Si)$_3$. Brazdova et al.[52] assigned the ~940 cm^{-1} band for vanadia supported on a thin alumina film to the V−O stretching in V−O−Al interface bonds using DFT calculations. Magg et al.[2] assigned a band at 926−955 cm^{-1} to ν_S(V−O) in V−O−Al and at 825−838 cm^{-1} to ν_{as}(V−O) in V−O−Al also using DFT calculations (model no. 9). Brazdova et al.[50] similarly assigned a band at 922 cm^{-1} to ν_S(V−O) and at 882 cm^{-1} to ν_{as}(V−O) by DFT calculations for the most stable structure of vanadia adsorbed on α-Al_2O_3. Finally, Le Coustumer et al. assigned a band at 915−943 cm^{-1} to ν_S(V−O) in VO_2 and at 905−910 cm^{-1} to ν_{as}(V−O) in VO_2 for VO_x on alumina based on Raman data and the correlation with other results reported for model compounds.[31] Our assignment is in good agreement with all of this prior work. The vibrational assignment, the observed wavenumbers and widths of the ν_1 progression, the width ratios (W_O/W_F), and the intensity ratios ($I_{2\nu 1}/I_{\nu 1}$) of the first overtone of ν_1 fundamental are given in Tables 3 and 4.

V−O Resonance Enhancement with 287 nm Excitation, Dehydrated. The 287 nm excitation is adjacent to an electronic band maximum at 265 nm (Figure 4). The Raman spectra (Figure 2, Table 4) from all dehydrated vanadia samples (0.16V, 1.2V, and 4.4V) are characterized by (1) a significant enhance-

TABLE 4: Observed Resonance Raman Data Excited at 220 and 287 nm for VO_x on θ-Alumina under the Dehydrated Conditions[a]

	0.16V			1.2V			4.4V		
		fwhm			fwhm			fwhm	
	position	220 nm	287nm	position	220 nm	287nm	position	220 nm	287nm
ν(V−O), A'' in C_s ν_S(V−O), A' in C_s	892 940	220	175	892 940	207	178	915 (892 and 940)	211	179
2ν(V−O) ν(V−O) + ν_S(V−O)	∼1805		265	1757		264	∼1805		266
$2\nu_S$(V−O) ν_S(V═O) + ν(V−O)	∼1870	279		∼1875	326		∼1830 ∼1895	337	
$3\nu_S$(V−O) $2\nu_S$(V═O)+ν(V−O)	∼2800 ∼2880			∼2800 ∼2885					
ratio of width relative to the width of fundamental		1.3	1.5		1.6	1.5		1.6	1.5

[a] Band position and fwhm (full width at half-maximum) are in cm^{-1}.

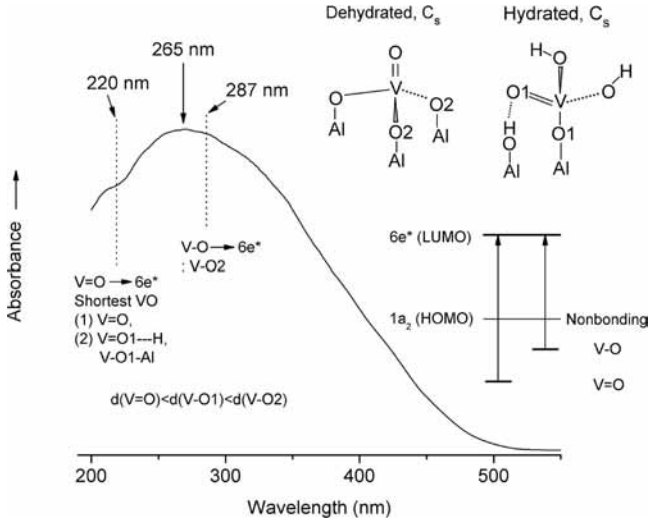

Figure 4. Selective resonance Raman enhancement associated with the two charge transfer bands at 210 and 265 nm for 0.16V, 1.2V, and 4.4V. The VO bonds having the shortest VO distance (i.e., terminal V═O under dehydrated conditions and V−O1 in V═O1···H and in V−O1−Al under hydrated conditions) are selectively resonant with the higher-energy excitation at 220 nm adjacent to 210 nm. The V−O bonds such as V−O2, longer than the shortest VO, are selectively resonant with the lower-energy excitation at 287 nm adjacent to 265 nm. The UV−vis absorption spectrum is reproduced from the published paper.[10] The relative electronic energies for V−O and V═O bonds are based on ref 73. The HOMO and LUMO symmetry were taken from ref 51. The degenerate symmetry of LUMO, e^*, is valid for only C_{3v} and is split into a' and a'' in C_s. The structures of C_{3v} (bidentate, Figure 5) and C_s (molecular) are not included because of the space limitation and can be found in ref 41.

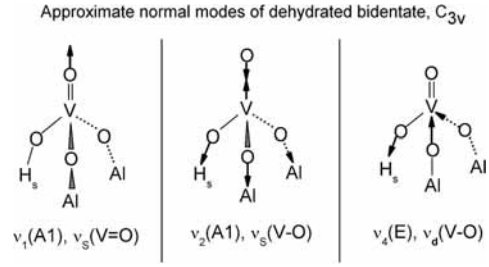

Figure 5. Approximate VO stretching normal modes of a monomeric vanadia on alumina for C_{3v} symmetry where basal oxygens are coordinated to Al and surface hydrogen. The subscripts s and d denote symmetric- and degenerate-stretching vibrations, respectively.[43]

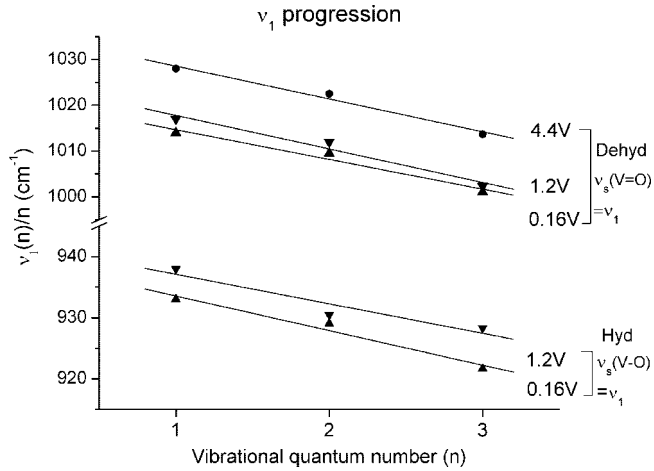

Figure 6. Plot of $\nu_1(n)/n$ versus n for the overtone progression observed in the resonance Raman spectra of dehydrated and hydrated vanadia on θ-alumina.

ment in the intensity of ν(V−O) and ν_S(V−O) fundamentals, (2) very weak overtones and combinations, and (3) the appearance of an overtone of 2ν(V−O) and a combination band of ν(V−O) + ν_S(V−O) that were not observed in the resonance Raman spectra excited at 220 nm.

The ν(V−O) and ν_S(V−O) fundamentals are typically very weak or undetected in nonresonance Raman spectra. The Raman intensity ratio of the overlapped V−O bands, ν(V−O) plus ν_S(V−O) to ν_S(V═O) fundamentals, $I_{V-O}/I_{V=O}$, in the spectra excited at 287 nm is about twice that observed for 220 nm excitation where the V−O fundamentals are strongly enhanced in intensity. It indicates that ν(V−O) and ν_S(V−O) modes are very strongly enhanced and selectively resonant with 287 nm excitation. The ratios of first overtone to fundamental intensity for ν_S(V═O) and ν(V−O) plus ν_S(V−O), $I_{2\nu 1}/I_{\nu 1}$ and $I_{2(\nu-O)}/I_{\nu-O}$, are very small (estimated ∼0.05 and ∼0.1, respectively). For comparison, $I_{2\nu 1}/I_{\nu 1}$ is in the range 0.3 to 0.5 in the resonance Raman spectra excited at 220 nm (Table 3). The $I_{2\nu}/I_{\nu}$ ratio is typically 0.2 to 0.7 and rarely exceeds ca. 0.7.[53] The theoretical maximum value for $I_{2\nu}/I_{\nu}$ at the resonance maximum is given by $\pi/4 = 0.79$ and $\pi/8 = \sim 0.4$ for a single displaced mode and for two equally displaced modes, respectively.[54]

Strong enhancement of the intensity of the totally symmetric fundamental, ν_S(V−O), combined with very weak overtones and combinations can be explained by the resonance enhancement through the A term[46,47] with a small displacement of the V−O bond length in the excited state,[19,21,23,28] a situation that is quite

common in polyatomic molecules.[28] The calculated V−O bond length change, as shown later, is much smaller than the V=O bond length change. An example of a very small bond length change in an excited electronic state can be V=O of V_2O_5. V_2O_5 strongly absorbs at both 220 and 287 nm.[55,56] The Raman fundamental band at 995 cm^{-1} in bulk V_2O_5 assigned[57,58] to the totally symmetric V=O stretching vibration (A_g) is quite intense with 220 or 287 nm excitation, but the first overtone at 1980 cm^{-1} is very weak with 220 nm excitation, $I_{2\nu 1}/I_{\nu 1} \approx 0.1$ (Figure 3, Table 3) and almost nonexistent with 287 nm excitation (Figure 2).

The appearance of 2ν(V−O) and the absence of $2\nu_S$(V−O) suggest that ν(V−O) is the most significantly enhanced leading mode with 287 nm excitation (Figure 2), which is similar to the progression-forming mode of ν_1 with 220 nm excitation (Figures 1, 3). The appearance of a combination, ν(V−O) + ν_S(V−O) band indicates that ν(V−O) and ν_S(V−O) modes are vibrationally coupled in the excited electronic state with 287 nm excitation (Figure 2, Table 4). An explanation of the enhancement mechanism for ν(V−O) follows.

A-term Enhancement Involving the Nontotally Symmetric V−O Mode with 287 nm: Jahn−Teller Distortion and Change of Symmetry in the Excited State. We assigned the ν(V−O) mode appearing at ∼892 cm^{-1} to the asymmetric ν_7 (A'') mode in C_s symmetry or ν_4 (E) in C_{3v} symmetry. Strong enhancement of fundamentals but very weak overtones of nonsymmetric (E, C_{3v} for CHX_3) and asymmetric C−X stretching (B_2, C_{2v} for CH_2X_2), where X is Cl and Br, has been observed in Raman spectra excited at 337 nm.[59] The symmetry species (E and B_2 vs E and A'') and the modes (C−X vs V−O) correlate nicely with our vibrational assignments.

The resonance Raman enhancement mechanisms of nontotally symmetric modes and totally symmetric modes are different. Although nontotally symmetric modes typically have no A-term contribution and do not show overtone progressions,[28] they can gain intensity in the fundamentals with either A-term or B-term resonance scattering. The B-term involves vibronic coupling of the resonant excited state to a second excited state and plays the dominant role only when the A term is zero because the B term is generally much smaller than the A term.[19] In practice, the B term becomes significant when the excitation wavelength is in a weakly allowed or forbidden region.[23,60,61] Because excitations at both 287 and 220 nm are in the strong absorption region, we can exclude the possibility of a B term or preresonance effect. Therefore, the enhancement of the nonsymmetric V−O fundamental at 892 cm^{-1} must be explained as A-term Raman scattering of nontotally symmetric modes.

The two possible mechanisms for this scattering are (1) the presence of Jahn−Teller (J−T) coupling in the resonant excited state and (2) a change in the molecular symmetry in this state.[19,21] Strong J−T distortion along an appropriate nontotally symmetric coordinate can produce significant Franck−Condon overlaps, that is, A term contributions.[28] If the excited state is degenerate and the nontotally symmetric vibration belongs to an irreducible representation contained in the direct product $\Gamma_e \otimes \Gamma_e$, where Γ_e is the orbital symmetry of the excited state, the nontotally symmetric mode will be J−T active and exhibit A-term activity.

For C_{3v} structures, the excited electronic state corresponds to the LUMO (lowest unoccupied molecular orbital), which is a degenerate, E-symmetry orbital.[51] In C_{3v}, the direct product is $E \otimes E = A_1 + [A_2] + E$, where the A_2 symmetry species given in square brackets is not J−T active.[21,43] Therefore, ν_4, the E-symmetry vibrational mode in C_{3v}, should be J−T active. The vibronic coupling between a J−T active nontotally symmetric mode and a totally symmetric mode results from a breakdown of the Condon approximation, which depends on the specifics of the modes.[62] The appearance of the combination ν_S(V−O) + ν_4 along with the first overtone of ν_4 is consistent with this interpretation, but the low intensity of these bands indicates that the J−T distortion is rather small.[19,21]

For C_s structures, the LUMO is nondegenerate. The orbital that has degenerate E symmetry in C_{3v} splits into $A' + A''$ when the symmetry is reduced to C_s. (See Table 1 or the correlation table[43,63] between C_{3v} and C_s.) In C_s symmetry, J−T coupling will be absent. In this case, the only mechanism for A-term Raman scattering of nontotally symmetric modes is a change of symmetry in the resonant excited state. If the C_s symmetry (tridentate or molecular) changes to C_{3v} (e.g., bidentate) in the excited state, the LUMO will have degenerate E symmetry from the merging of A' and A''. The asymmetric ν_7 (A'') vibration and the symmetric ν_3 (A') stretch in C_s will merge into the degenerate ν_4(E) mode in C_{3v}. (See Table 1.) This could result in J−T coupling. Examples of higher symmetry in the excited state reported in the literatures include H_3O^+ (D_{3h} from C_{3v} in the ground state)[64] and HCO, H_2O^+, NO_2, and so on (linear from bent in the ground state).[65] Alternatively, the structure could simply follow the second mechanism, which requires a change to lower symmetry (e.g., C_1) in the excited state.

V=O···H Resonance Enhancement with 220 nm Excitation, Hydrated. Resonance Raman spectra excited at 220 nm for 0.16V, 1.2V, and 4.4V under hydrated conditions (Figure 3) are characterized by (1) the absence of terminal V=O stretching bands in the ∼990−1050 cm^{-1} region, except for the 995 cm^{-1} band at 4.4V due to V=O of V_2O_5, (2) the appearance of an intense ν_1 fundamental at ∼938 cm^{-1} and its overtones, $2\nu_1$ and $3\nu_1$, (3) the appearance of V−O stretching vibrations as a weak shoulder, ν(V−O), centered at ∼850 cm^{-1}, (4) the appearance of a combination progression in ν_1 + ν(V−O), and (5) the disappearance of a 3728 cm^{-1} band that has been assigned[66] to terminal OH vibrations in Al−OH, concomitant with the appearance of a broad Raman band centered at ∼3490 cm^{-1} and assigned[67] to hydrogen-bonded OH stretching vibrations. The highest-frequency VO stretching vibration is defined as ν_1. Therefore, the ∼938 cm^{-1} band is designated ν_1 and is equivalent to ν_S(V−O) under hydrated conditions where V=O is absent. We will not discuss point 5 in this article because it has been explained elsewhere.[41]

Vibrational Assignment. The appearance of first and second overtones of the ∼938 cm^{-1} band, ν_1 (Figure 3) demonstrates that it is a totally symmetric mode, as explained above. DFT calculations[41] for the most stable structure under hydrated conditions obtained a monodentate structure (C_s symmetry) consisting of two long V−O lengths of 1.72 and 1.82 Å for V−OH's and two short V−O's (1.66 to 1.67 Å) in V−O−Al and V=O···H. Three totally symmetric V−O stretching vibrations corresponding to the three V−O lengths are expected from C_s symmetry. (See Table 1.) As the highest frequency band at ∼990−1050 cm^{-1} is assigned to ν_S(V=O), associated with the shortest VO bond under dehydrated conditions, we similarly assign the highest frequency ν_1 band at ∼938 cm^{-1} to ν_S(V−O), associated with the shortest V−O bond of 1.66 to 1.67Å with A' symmetry in the C_s point group (Tables 1 and 3). The ν_1 band includes a 933 cm^{-1} band for 0.16V, a 938 cm^{-1} band for 1.2V, and a 943 cm^{-1} band for 4.4V. The ν_1, ν_S(V−O), as well as the ν_1, ν_S(V=O), bands under dehydrated conditions shift to higher wavenumber as the vanadia surface density increases.

The ~850 cm^{-1} band, ν(V−O), can be assigned to the symmetric V−O stretching vibrations associated with the V−O bond length of 1.72 Å or to the asymmetric V−O vibrations. On the basis of the absence of the overtones of ν(V−O), it is more likely due to the asymmetric V−O stretching vibrations (ν_7, A'' in C_s, monodentate).

A combination progression of $\nu_1 + \nu$(V−O) induced by the progression-forming ν_1 mode is obvious in the resonance Raman spectra up to $2\nu_1 + \nu$(V−O) (Figure 3). Interestingly, the same type of $\nu_1 + \nu$(V−O) combination bands and ν_1 overtones strongly appears with 220 nm excitation under dehydrated or hydrated conditions. The only difference between the two cases is a redshift in ν_1 and ν(V−O) under hydrated conditions. Because the leading, progression-forming ν_1 mode is the highest-frequency VO stretching vibration, the observation implies that 220 nm excitation is associated with the selective enhancement of the highest-frequency VO stretch, as discussed later.

Reversible Shift of V═O between Hydrated and Dehydrated Conditions. Under hydrated conditions, the absence of terminal V═O bands centered near 1020 cm^{-1} coupled to the appearance of the ~938 cm^{-1} band has been previously reported for vanadia supported on alumina by Raman spectroscopy.[68] Similar Raman results were observed for ReO_x, MoO_x, and WO_x supported on alumina. In all cases, structural transformations responsible for the two distinct Raman bands are reversible with repeated dehydration and hydration treatments.[39,40,69] The possible structures for hydrated VO_x on alumina have been studied less thoroughly than those for dehydrated VO_x.[9] Went et al. proposed[70] a structural model for VO_x on alumina that involves coordination of water to V atoms of $O{=}VO_3$, resulting in five- or six-coordinated structures. This coordination mechanism is unlikely for VO_x on alumina, especially at low V surface coverage, because the structures still have slightly distorted tetrahedral coordination, as confirmed by EXAFS and ^{51}V NMR spectra.[32,34,36] The five- or six-coordinated structural model[71] for hydrated VO_x, which seems to be valid on SiO_2, should not be applied to VO_x on alumina.

Stencel et al.[39,40] explained the transformation in terms of a reversible shift produced by an increased bond length and decreased bond order for hydrated M═O (M = Mo, W) following the smooth, monotonic relationship among the bond length, bond order, and stretching force constant reported by Cotton and Wing.[72] The tetrahedral model including the formation of M═O···H bonds is reasonable for hydrated VO_x on alumina at the low V concentration limit. The lengthening of the V═O bond for hydrated VO_x on alumina to 1.67 Å has been reported by EXAFS.[32] This is in excellent agreement with the bond lengths of 1.66 and 1.67 Å calculated by DFT[41] for the two shortest V−O bonds, where one is V═O with the oxygen atom coordinated to surface hydrogen in Al−OH and the other is V−O in V−O−Al, respectively. One report of a short 1.58 Å bond length by Keller et al.[36] for hydrated VO_x on alumina is less reliable because the bond length was fixed during the EXAFS fitting process. By comparison, the V═O bond length for dehydrated VO_x on alumina has been reported to be 1.58 Å by EXAFS[35] and DFT calculations.[41] Therefore, the absence of terminal V═O stretching bands appearing in the ~990−1050 cm^{-1} region and the appearance of the intense band at ~938 cm^{-1} under hydrated conditions (Figure 3) can be explained by an elongated V═O bond in a distorted VO_4 tetrahedral structure.

Bond Length Change in the Excited State for V═O and Elongated V═O in V═O···H and V−O−Al. Using Raman excitation profiles for the observed fundamental and overtones, the change in V═O bond length in the excited state compared with that in the ground state, Δr, can be estimated from the displacement along the normal coordinate ($\Delta Q_k = \mu^{1/2}\Delta S$) and along the symmetry coordinate ($\Delta S = \Delta r$ for V═O), the reduced mass (μ) associated with the V═O vibration, and the dimensionless shift parameter, $\Delta_k \approx 0.5$. Δ_k is defined by $(\pi\nu_k/\hbar)^{1/2}\Delta Q_k$ where $\hbar$ is Planck's constant and ν_k is the V═O stretching frequency.[19,21] A value of $\Delta r \approx 0.09$ Å for the V═O vibration at 1014 cm^{-1} of dehydrated vanadia is obtained from the spectra excited at 220 nm. A little larger value for Δr is expected for excitation at the absorption band maximum of ~210 nm. The value 0.09 Å is close to the value 0.12 to 0.14 Å obtained by Franck−Condon analysis of the VO_x emission spectrum.[51] For comparison, $\Delta r \approx 0.3$ Å was obtained theoretically for the V═O vibration in free $O{=}V(OH)_3$.[73]

The change in elongated V═O (or V═O···H) length for the excited state can also be estimated from the 220 nm excited Raman band at 938 cm^{-1}. A value of ~0.06 Å for each V−O bond was obtained using the relationship described above but using a different molecular type of VO_2, a different symmetry coordinate, and a different reduced mass, $\Delta S = 2^{1/2}\Delta r$ and $\mu = m_o$, where m_o is the mass of oxygen.

The change in V−O length for the excited state was also estimated from the 287 nm excited Raman band at 940 cm^{-1} using a smaller shift parameter of $\Delta_k = 0.1$. Values of 0.01 and 0.02 Å for each V−O bond were obtained for tridentate and molecular structures, respectively.

Selective Resonance Raman enhancement of V═O and V−O, Charge Transfer Band Assignment, and the Correlation of E_{CT} to the VO Bond Length. All of the hydrated and dehydrated vanadia samples show two charge-transfer band maxima centered around 210 and 265 nm in the UV−vis absorption spectra (Figure 4). The 4.4V spectrum exhibits an additional charge-transfer band maximum centered near 320 nm (not shown in Figure 4) that tails into the visible region with significant absorption at 430 nm.[10] The spectrum from 1.2V shows quite strong absorption at 320 nm but weak absorption in the 430 nm region.[10]

An empirical linear correlation has been established between the absorption edge energy appearing in the 354−564 nm region and the number of V−O−V bonds (i.e., degree of polymerization) using model compounds having zero to five V−O−V bonds.[56,71] Another empirical (inversely proportional) correlation of the lower-energy charge-transfer band maximum in the 290−467 nm region for VO_x on silica to the coordination number has been found using model compounds with coordination numbers between four and six.[74] UV−vis spectral features for vanadia on silica and on alumina are similar, but the two charge-transfer band maxima for alumina are somewhat higher in energy, ~210 and ~265 nm for VO_x on alumina and ~250 and ~290 nm for VO_x on silica. Therefore, on alumina, the 265 nm band corresponds to the lower-energy charge-transfer band. According to the correlation, the bands centered at 265, 320, and ~430 nm in the UV−vis spectra for 0.16V, 1.2V, and 4.4V correspond to monomeric tetrahedral, four- or five-coordinate, and five- or six-coordinate structures, respectively.

The higher-energy charge transfer band has not been identified. We assign the higher-energy and lower-energy charge transfer bands to the V═O (shortest VO) and V−O (longer than the shortest VO) transitions on the basis of the selective resonance Raman enhancement of the V═O and V−O vibrations with 220 and 287 nm excitation. The selective enhancement of different vibrational modes with different excitation

wavelengths is illustrated in Figure 4, and similar observations have been reported for other species such as water and biological compounds.[23,75−77] Consistent with this picture, molecular orbital calculations for the VO_4H_3 cluster showed that the orbitals associated with V=O bonds are lower in energy than those for V−O bonds (Figure 4),[73] and Arena et al. assigned the higher-energy charge transfer band observed at ∼40 000 cm^{-1} (250 nm) for VO_x on silica to the terminal V=O bond.[78]

The calculated[79] charge transfer energy, E_{CT}, in the region 243−335 nm as a function of the VO bond length, R_{VO}, in the range 1.65 to 1.82 Å for tetrahedral VO_4^{3-} can be fitted to a linear equation with E_{CT} in nm and R_{VO} in Å: $R_{VO} = 1.224 + 0.00174\ E_{CT}$. This relation can be extended to the shorter VO bond lengths corresponding to V=O in C_{3v} or C_s symmetry because the V=O stretching mode involves negligible movement of other atoms in the VO_4 unit.[43,80] Extrapolation of the equation to shorter and longer VO regions produces an excellent agreement with both our V=O assignment and the correlation[74] with the lower-energy charge-transfer band. The ∼210 nm band corresponds to a VO bond length of 1.59 Å which is very close to the typical terminal V=O bond length of 1.58 Å. The 265, 320, and 430 nm bands correspond to VO bond lengths of 1.69, 1.78, and 1.97 Å, respectively, which match well with the average VO length in four-coordinate (1.69 to 1.74 Å), five-coordinate (1.79 to 1.9 Å), and six-coordinate (1.96 to 1.99 Å) vanadium oxide reference compounds taken from ref 81. The equation is also consistent with the linear relationship between E_{CT} and the totally symmetric ν_1 frequency of tetrahedral oxo-, thio-, and seleno-anions,[82,83] the monotonic relationship between R_{VO} (including V=O), and the position of the highest-frequency, ν_1, Raman band.[52,81,84]

For hydrated VO_x, where the V=O vibration is absent, the highest-frequency V−O vibration, centered at ∼938 cm^{-1}, showed strong resonance enhancement with 220 nm excitation. The above correlation suggests that the ∼938 cm^{-1} band should be associated with the shortest V−O bond among the various possibilities for hydrated VO_x, V−O−Al, and V−O−H, and so on, which is consistent with our vibrational assignment. These observations are in conflict with the previous assignment of the 385 nm (26 000 cm^{-1}) charge-transfer band to V=O.[85]

Width of Overtone Bands. The V=O first overtone bands are broader than the fundamental bands by approximately 30−50% (Table 3). Similar broadening of overtone Raman bands in metal oxide ions has been reported in the literature. For example, Kiefer and Bernstein[48] observed the first overtone band of the totally symmetric (ν_1, A_1) vibration in CrO_4^{2-} to be broader than the fundamental band by 67%. In general, first overtones are broader in width than fundamentals, and second overtones are broader than first overtones.[53]

The main sources of vibrational band broadening are inhomogeneous broadening due to different molecular environments, the vibrational relaxation time associated with excited-state decay, and the dephasing time associated with the loss of phase coherence in the excited vibrations.[86] Because the environmental effects influencing fundamental and overtone vibrations are identical, the observed broadening of V=O overtone bands is most likely due to faster excited-state decay (either relaxation or dephasing). The vibrational dephasing time can be obtained experimentally (e.g., by coherent anti-Stokes Raman).[86] When extended overtone progressions are available experimentally, the dependence of overtone width on overtone order can be used to distinguish energy relaxation from vibrational frequency modulation on the basis of the relationship between overtone width with the parameters affecting it.[87]

Anharmonic Constants and Dissociation Energy. ***Harmonic wavenumber and Anharmonic Constant.*** The observation of first and second overtones in ν_1 vibrations allows the determination of both the harmonic wavenumber, ω_e, and anharmonic constant $\omega_e x_e$ ($= x_{mm}$). ω_e ($= \omega_m$) is the vibrational frequency corrected for anharmonicity and represents the frequency associated with infinitely small vibrations about the equilibrium separation in the actual potential field (anharmonic oscillator).[19,42] The observed wavenumbers, $\nu_m(n)$, for fundamental ($n = 1$), first overtone ($n = 2$), and second overtone ($n = 3$) from a polyatomic anharmonic oscillator are given[28,53] by the expression $\nu_m(n) = n\omega_m - n(n+1)x_{mm} + ...$, where m is the normal mode identifier, for example, ω_1 and x_{11} for the ν_1 mode and ω_2 and x_{22} for the ν_2 mode. A plot of $\nu_m(n)/n$ versus n should be a straight line of slope x_{mm} and an intercept, which gives $\omega_m - x_{mm}$ and thus ω_m. Plots of the overtone progressions in ν_1 and ν_S(V−O) (Figures 1 and 3) are shown in Figure 6. The values of ω_m and x_{mm} determined by the plot for each sample are included in Table 3. Values for ω_1 and x_{11} may also be obtained from the $n\nu_1 + \nu$(V−O) combination progression by plotting $[(n\nu_1 + \nu(V-O)) - \nu(V-O)]/n$ versus n, but the results are less accurate because of the small number of data points and the difficulty in determining the position of broad bands.

The x_{11} values of 6.5 to 7.3 cm^{-1} obtained from the plot are slightly larger than 5 to 5.5 cm^{-1} obtained from using only the fundamental and first overtone bands for 0.16V, 1.2V, and 4.4V. The range 5 to 5.5 cm^{-1} is in good agreement with the 5 cm^{-1} value estimated from the reported[7,88] IR V=O bands at 1026 and 2042 cm^{-1} for 5% V_2O_5/γ-Al_2O_3 and with the 4.9 cm^{-1} value for diatomic V=O.[89]

The values are significantly smaller than those obtained from either a higher loading vanadia or a different support. The x_{11} value of 12.5 cm^{-1} can be estimated from the IR bands at 1030 and 2035 cm^{-1} for 5% V_2O_5/TiO_2[17] or at 1035 and 2045 cm^{-1} for 9% V_2O_5/TiO_2.[90] A x_{11} value of 17.5 cm^{-1} can also be estimated from the IR bands at 1036 and 2037 cm^{-1} for 20% V_2O_5/Al_2O_3[17].[7,13,88,89] This range in measured values for x_{11} indicates that the anharmonicity is sensitive, not surprisingly, to the environment of the V=O oscillator. For example, the influence of the environment on the value of x_{11} for I_2 stretching caused by different solvents was almost a factor of two.[91]

Among the previous reports, the low-loading VO_x material is the most similar to our samples, and the reported value is the closest to ours. It should also be pointed out that the additional data points obtained from a longer overtone progression makes it possible to obtain more accurate anharmonic constants. Kiefer et al.[91] obtained precise anharmonic constants for I_2 from very long overtones up to the 14th, whereas using only two data points gives somewhat deviated values.

Anharmonic Force Constants. The force constant is representative of the curvature at the bottom of ground-state potential curve, and the value has significance in many applications, for example, the correlation between the force constant and bond length,[72,92] the relationship between force constant and activation energy[93] or dissociation energy (see below), and the calculation of kinetic isotope effects in the catalytic reaction.[94] The anharmonicity-corrected force constant, f_e, called the anharmonic force constant, can be obtained using the diatomic oscillator approximation from the equation $\omega_e = 0.5(\pi c)^{-1}\sqrt{f_e/\mu}$, where μ is the reduced mass and ω_e is harmonic wavenumber. f_e is, in theory, a more exact representation of the bond force constant than f obtained from the harmonic oscillator equation given by $\omega = 0.5(\pi c)^{-1}\sqrt{f/\mu}$, where ω is the wavenumber observed from IR or Raman spectra. [42,43,63]

The force constants for V=O obtained from this equation are expected to be quite accurate because the V=O stretching mode in C_{3v} symmetry involves no significant motion of the other atoms in the VO_4 unit.[43,80] The force constants for ν_S(V−O) are likely to be less accurate than V=O force constants because ν_S(V−O) mode partially includes the movement of V=O. (See Figure 5.)[43] A more accurate estimate can be performed using the effective reduced mass μ_{eff} rather than the diatomic reduced mass of μ.[95] The anharmonic and harmonic force constants for ν_S(V=O) and ν_S(V−O) obtained from the resonance Raman data are included in Table 3 and are compared with the published force constants for ν_S(V=O).[72] The measured values of V=O and V−O force constants match well with the general trend f(V=O) > f(V−O).

Dissociation Energy. The dissociation energy along a normal coordinate, D_0, is the sum of the vibrational levels of the anharmonic oscillator and represents the depth of the vibrational potential well below the dissociation limit. It can be calculated from the harmonic frequency, ω_m, and anharmonic constant, x_{mm}, using the standard equation for an anharmonic oscillator by neglecting cubic and higher-order terms: D_0 (in cm^{-1}) = $(0.25\ \omega_m^2/x_{mm}) - (\omega_m/2) + (x_{mm}/4)$, where $(\omega_m/2) - (x_{mm}/4)$ is the zero point energy.[80]

The D_0 (kJ/mol) values for ν_S(V=O) and ν_S(V−O) modes determined from the resonance Raman spectra are included in Table 3. The average D_0 value estimated for ν_S(V=O) is ∼450 kJ/mol. For comparison, the reported D_0 for diatomic V=O is 600−640 kJ/mol.[89,96] The value ∼450 kJ/mol is in good agreement with the value ∼450−460 kJ/mol for ν_S(V=O) in vanadia supported on alumina from the DFT calculations with periodic boundary conditions (PW91)[58] and is in reasonable agreement with the values 301−393 kJ/mol for a supported-alumina model cluster O=VAl_7O_{12} calculated by DFT with three different functionals.[97] It is interesting to note that 1.2V shows the lowest bond dissociation energy for ν_S(V=O) and ν_S(V−O) among the samples studied. This may be relevant to the catalytic performance of 1.2V for the butane hydrogenation relative to the other samples.[98]

Summary

Resonance Raman spectroscopic results for vanadia supported on θ-alumina excited at 220 and 287 nm have been described and extensively discussed. To our knowledge, this work is the first detailed resonance Raman analysis applied to solid metal oxide catalysts.

From the analysis of fundamentals, overtones, and combinations observed in the resonance Raman spectra, several findings include (1) the estimation of in situ V=O bond dissociation energy, which could be significant for catalytic bond-breaking and -making processes, (2) distinguishing symmetric V−O stretching from nonsymmetric V−O stretching in the Raman spectra, (3) estimation of anharmonic constants and anharmonic force constants for V=O and symmetric V−O stretching modes, (4) estimation of V=O and V−O bond length changes in the excited electronic state, (5) assignment of V=O and V−O charge transfer bands, and (6) observation of a simple, empirical equation that can be used to assign the charge-transfer bands and to estimate the V=O and V−O bond length (and coordination number) from UV−vis spectra.

Acknowledgment. H.-S.K. thanks Dr. Zili Wu for supplying the samples used in the published paper.[10] This work was performed at Argonne National Laboratory supported by the U.S. Department of Energy, BES-Chemical Sciences under contract W-31-109-ENG-38.

References and Notes

(1) Keller, D. E.; Koningsberger, D. C.; Weckhuysen, B. M. *J. Phys. Chem. B* **2006**, *110*, 14313.
(2) Magg, N.; Immaraporn, B.; Giorgi, J. B.; Schroeder, T.; Baumer, M.; Dobler, J.; Wu, Z. L.; Kondratenko, E.; Cherian, M.; Baerns, M.; Stair, P. C.; Sauer, J.; Freund, H. J. *J. Catal.* **2004**, *226*, 88.
(3) Stencel, J. M. *Raman Spectroscopy for Catalysis*; Van Nostrand Reinhold: New York, 1990.
(4) Busca, G. *J. Raman Spectrosc.* **2002**, *33*, 348.
(5) Wachs, I. E. *Catal. Today* **2005**, *100*, 79.
(6) Weckhuysen, B. M.; Keller, D. E. *Catal. Today* **2003**, *78*, 25.
(7) Wachs, I. E. *Catal. Today* **1996**, *27*, 437.
(8) Khodakov, A.; Olthof, B.; Bell, A. T.; Iglesia, E. *J. Catal.* **1999**, *181*, 205.
(9) Banares, M. A.; Wachs, I. E. *J. Raman Spectrosc.* **2002**, *33*, 359.
(10) Wu, Z. L.; Kim, H. S.; Stair, P. C.; Rugmini, S.; Jackson, S. D. *J. Phys. Chem. B* **2005**, *109*, 2793.
(11) Zhao, Z.; Liu, J.; Duan, A.; Xu, C.; Kobayashi, T.; Wachs, I. E. *Top. Catal.* **2006**, *38*, 309.
(12) Krishnan, R. S. Chapter 1, Historical Introduction. In *The Raman Effect*; Anderson, A., Ed.; Marcel Dekker, Inc: New York, 1971; Vol. 1.
(13) Miller, F. A.; Cousins, L. R. *J. Chem. Phys.* **1957**, *26*, 329.
(14) Busca, G. *Mater. Chem. Phys.* **1988**, *19*, 157.
(15) Topsøe, N.-Y. *J. Catal.* **1991**, *128*, 499.
(16) Rice, G. L.; Scott, S. L. *J. Mol. Catal. A: Chem.* **1997**, *125*, 73.
(17) Burcham, L. J.; Deo, G.; Gao, X.; Wachs, I. E. *Top. Catal.* **2000**, *11/12*, 85s.
(18) Lee, E. L.; Wachs, I. E. *J. Phys. Chem. C* **2008**, *112*, 6487.
(19) Long, D. A. *The Raman Effect: A Unified Treatment of the Theory of Raman Scattering by Molecules*; Wiley: New York, 2002.
(20) Kiefer, W. *Appl. Spectrosc.* **1974**, *28*, 115.
(21) Clark, R. J. H.; Dines, T. J. *Angew. Chem., Int. Ed. Engl.* **1986**, *25*, 131.
(22) Asher, S. A. *Annu. Rev. Phys. Chem.* **1988**, *39*, 537.
(23) Spiro, T. G.; Czernuszewicz, R. S. 2. Resonance Raman Spectroscopy. In *Physical Methods in Bioinorganic Chemistry: Spectroscopy and Magnetism*; Que, L., Jr., Ed.; University Science Books: Sausalito, CA, 2000.
(24) Stair, P. C.; Li, C. *J. Vac. Sci. Technol., A* **1997**, *15*, 1679.
(25) Stair, P. C. *Adv. Catal.* **2007**, *51*, 75.
(26) Xiong, G.; Li, C.; Feng, Z.; Ying, P.; Xin, Q.; Liu, J. *J. Catal.* **1999**, *186*, 234.
(27) Li, C. *J. Catal.* **2003**, *216*, 203.
(28) Clark, R. J. H.; Stewart, B. *Struct. Bonding (Berlin, Ger.)* **1979**, *36*, 1.
(29) Lever, A. B. P. *Inorganic Electronic Spectroscopy*, 2nd ed.; Elsevier: New York, 1984.
(30) Chua, Y. T.; Stair, P. *J. Catal.* **2000**, *196*, 66.
(31) Le Coustumer, L. R.; Taouk, B.; Le Meur, M.; Payen, E.; Guelton, M.; Grimblot, J. *J. Phys. Chem.* **1988**, *92*, 1230.
(32) Tanaka, T.; Yamashita, H.; Tsuchitani, R.; Funabiki, T.; Yoshida, S. *J. Chem. Soc., Faraday Trans. 1* **1988**, *84*, 2987.
(33) Yoshida, S.; Tanaka, T.; Nishimura, Y.; Mizutani, H.; Funabiki, T. *Proc. Int. Congr. Catal., 9th* **1988**, *3*, 1473.
(34) Eckert, H.; Wachs, I. E. *J. Phys. Chem.* **1989**, *93*, 6796.
(35) Keller, D. E.; de Groot, F. M. F.; Koningsberger, D. C.; Weckhuysen, B. M. *J. Phys. Chem. B* **2005**, *109*, 10223.
(36) Keller, D. E.; Koningsberger, D. C.; Weckhuysen, B. M. *Phys. Chem. Chem. Phys.* **2006**, *8*, 4814.
(37) Kobayashi, H.; Yamaguchi, M.; Tanaka, T.; Nishimura, Y.; Kawakami, H.; Yoshida, S. *J. Phys. Chem.* **1988**, *92*, 2516.
(38) Ruitenbeek, M.; Van Dillen, A. J.; de Groot, F. M. F.; Wachs, I. E.; Geus, J. W.; Koningsberger, D. C. *Top. Catal.* **2000**, *10*, 241.
(39) Stencel, J. M.; Makovsky, L. E.; Sarkus, T. A.; De Vries, J.; Thomas, R.; Moulijn, J. A. *J. Catal.* **1984**, *90*, 314.
(40) Stencel, J. M.; Makovsky, L. E.; Diehl, J. R.; Sarkus, T. A. *J. Raman Spectrosc.* **1984**, *15*, 282.
(41) Kim, H.-S.; Zygmunt, S. A.; Stair, P. C.; Zapol, P.; Curtiss, L. A. *J. Phys. Chem. C*, submitted.
(42) Herzberg, G. *Spectra of Diatomic Molecules*, 2nd ed.; D. van Nostrand Company, Inc: New York, 1950; Vol. 1.
(43) Nakamoto, K. *Infrared and Raman Spectra of Inorganic and Coordination Compounds, Part A: Theory and Applications in Inorganic Chemistry*, 5th ed.; John Wiley & Sons, Inc.: New York, 1997.
(44) Wu, Z.; Kim, H.-S.; Stair, P. C. Resonance Raman Spectroscopy -θ-Al_2O_3-Supported Vanadium Oxide Catalysts as an Illustrative Example. In *Metal Oxide Catalysis*; Jackson, S. D., Hargreaves, J. S. J., Eds.; Wiley-VCH: Weinheim, Germany, 2008; Vol. 1, p 177.
(45) Cortez, G. G.; Banares, M. A. *J. Catal.* **2002**, *209*, 197.
(46) Albrecht, A. C. *J. Chem. Phys.* **1961**, *34*, 1476.

(47) Tang, J.; Albrecht, A. C. Developments in the Theories of Vibrational Raman Intensities. In *Raman Spectroscopy*; Szymanski, H. A., Ed.; Plenum: New York, 1970; Vol. 2, p 33.
(48) Kiefer, W.; Bernstein, H. J. *Mol. Phys.* **1972**, *23*, 835.
(49) Bosworth, Y. M.; Clark, R. J. H. *Chem. Phys. Lett.* **1974**, *28*, 611.
(50) Brazdova, V.; Ganduglia-Pirovano, M. V.; Sauer, J. *J. Phys. Chem. B* **2005**, *109*, 23532.
(51) Tran, K.; Hanning-Lee, M. A.; Biswas, A.; Stiegman, A. E.; Scott, G. W. *J. Am. Chem. Soc.* **1995**, *117*, 2618.
(52) Brazdova, V.; Ganduglia-Pirovano, M. V.; Sauer, J. *J. Phys. Chem. B* **2005**, *109*, 394.
(53) Clark, R. J. H. Resonance Raman Spectra of Inorganic Molecules and Ions. In *Advances in Infrared and Raman Spectroscopy*; Clark, R. J. H., Hester, R. E., Eds.; Heyden: New York, 1975; Vol. 1, p 143.
(54) Heller, E. J.; Sundberg, R.; Tannor, D. *J. Phys. Chem.* **1982**, *86*, 1822.
(55) Schraml-Marth, M.; Wokaun, A.; Baiker, A. *J. Catal.* **1990**, *124*, 86.
(56) Gao, X. T.; Wachs, I. E. *J. Phys. Chem. B* **2000**, *104*, 1261.
(57) Abello, L.; Husson, E.; Repelin, Y.; Lucazeau, G. *Spectrochim. Acta, Part A* **1983**, *39A*, 641.
(58) Brazdova, V.; Ganduglia-Pirovano, M. V.; Sauer, J. *Phys. Rev. B: Condens. Matter Mater. Phys.* **2004**, *69*, 165420/1.
(59) Kaya, K.; Mikami, N.; Udagawa, Y.; Ito, M. *Chem. Phys. Lett.* **1972**, *13*, 221.
(60) Mishra, T.; De, A. K.; Chattopadhyay, S.; Mallick, P. K.; Sett, P. *Spectrochim. Acta, Part A* **2005**, *61*, 767.
(61) Smith, E.; Dent, G. *Modern Raman Spectroscopy: A Practical Approach*; J. Wiley: Hoboken, NJ, 2005.
(62) Samoc, M.; Siebrand, W.; Williams, D. F.; Woolgar, E. G.; Zgierski, M. Z. *J. Raman Spectrosc.* **1981**, *11*, 369.
(63) Harris, D. C.; Bertolucci, M. D. *Symmetry and Spectroscopy: An Introduction to Vibrational and Electronic Spectroscopy*; Dover Publications: New York, 1978.
(64) Klein, S.; Kochanski, E.; Strich, A. *Chem. Phys. Lett.* **1996**, *260*, 34.
(65) Bersuker, I. B. *The Jahn-Teller Effect*; Cambridge University Press: New York, 2006.
(66) Kubicki, J. D.; Apitz, S. E. *Am. Mineral.* **1998**, *83*, 1054.
(67) McDonald, R. S. *J. Phys. Chem.* **1958**, *62*, 1168.
(68) Chan, S. S.; Wachs, I. E.; Murrell, L. L.; Wang, L.; Hall, W. K. *J. Phys. Chem.* **1984**, *88*, 5831.
(69) Wang, L.; Hall, W. K. *J. Catal.* **1983**, *82*, 177.
(70) Went, G. T.; Oyama, S. T.; Bell, A. T. *J. Phys. Chem.* **1990**, *94*, 4240.
(71) Gao, X.; Bare, S. R.; Weckhuysen, B. M.; Wachs, I. E. *J. Phys. Chem. B* **1998**, *102*, 10842.
(72) Cotton, F. A.; Wing, R. M. *Inorg. Chem.* **1965**, *4*, 867.
(73) Kobayashi, H.; Yamaguchi, M.; Tanaka, T.; Yoshida, S. *J. Chem. Soc., Faraday Trans. 1* **1985**, *81*, 1513.
(74) Schraml-Marth, M.; Wokaun, A.; Pohl, M.; Krauss, H. L. *J. Chem. Soc., Faraday Trans.* **1991**, *87*, 2635.
(75) Mayer, E.; Gardiner, D. J.; Hester, R. E. *Mol. Phys.* **1973**, *26*, 783.
(76) Czernuszewicz, R. S.; LeGall, J.; Moura, I.; Spiro, T. G. *Inorg. Chem.* **1986**, *25*, 696.
(77) Sension, R. J.; Brudzynski, R. J.; Hudson, B. S. *Phys. Rev. Lett.* **1988**, *61*, 694.
(78) Arena, F.; Frusteri, F.; Martra, G.; Coluccia, S.; Parmaliana, A. *J. Chem. Soc., Faraday Trans.* **1997**, *93*, 3849.
(79) Ronde, H.; Snijders, J. G. *Chem. Phys. Lett.* **1977**, *50*, 282.
(80) Herzberg, G. *Infrared and Raman Spectra of Polyatomic Molecules*; Van Nostrand: New York, 1945; Vol. 2.
(81) Hardcastle, F. D.; Wachs, I. E. *J. Phys. Chem.* **1991**, *95*, 5031.
(82) Kebabcioglu, R.; Müller, A.; Rittner, W. *J. Mol. Struct.* **1971**, *9*, 207.
(83) Kebabcioglu, R.; Müller, A. *Chem. Phys. Lett.* **1971**, *8*, 59.
(84) Asmis, K. R.; Meijer, G.; Bruemmer, M.; Kaposta, C.; Santambrogio, G.; Woeste, L.; Sauer, J. *J. Chem. Phys.* **2004**, *120*, 6461.
(85) Centi, G.; Perathoner, S.; Trifiro, F.; Aboukais, A.; Aissi, C. F.; Guelton, M. *J. Phys. Chem.* **1992**, *96*, 2617.
(86) Clarke, J. H. R. Band shapes and molecular dynamics in liquids. In *Advances in Infrared and Raman Spectroscopy*; Clark, R. J. H., Hester, R. E., Eds.; Heyden: New York, 1978; Vol. 4, p 109.
(87) Battaglia, M. R.; Madden, P. A. *Mol. Phys.* **1978**, *36*, 1601.
(88) Vuurman, M. A.; Stufkens, D. J.; Oskam, A.; Deo, G.; Wachs, I. E. *J. Chem. Soc., Faraday Trans.* **1996**, *92*, 3259.
(89) Huber, K. P.; Herzberg, G. *Molecular Spectra and Molecular Structure, 4: Constants of Diatomic Molecules*; Van Nostrand: New York, 1979.
(90) Busca, G.; Lavalley, J. C. *Spectrochim. Acta, Part A* **1986**, *42*, 443.
(91) Kiefer, W.; Bernstein, H. J. *J. Raman Spectrosc.* **1973**, *1*, 417.
(92) Badger, R. M. *J. Chem. Phys.* **1934**, *2*, 128.
(93) Denisov, E. T.; Afanas'ev, I. B. *Oxidation and Antioxidants in Organic Chemistry and Biology*; Taylor & Francis: Boca Raton, FL, 2005.
(94) Kobal, I.; Burghaus, U.; Senegacnik, M.; Ogrinc, N. *J. Phys. Chem. B* **1998**, *102*, 6787.
(95) Dong, S.; Padmakumar, R.; Banerjee, R.; Spiro, T. G. *Inorg. Chim. Acta* **1998**, *270*, 392.
(96) Berkowitz, J.; Chupka, W. A.; Inghram, M. G. *J. Chem. Phys.* **1957**, *27*, 87.
(97) Sauer, J.; Doebler, J. *Dalton Trans.* **2004**, 3116.
(98) Wu, Z.; Stair, P. C. *J. Catal.* **2006**, *237*, 220.

JP811019C